

Localized Delivery of Antisense Oligonucleotides by Cationic Hydrogel Suppresses TNF- α Expression and Endotoxin-Induced Osteolysis

Lei Dong · Zhen Huang · Xing Cai · Jiawei Xiang · Yi-An Zhu · Rui Wang · Jiangning Chen · Junfeng Zhang

Received: 30 September 2010 / Accepted: 17 November 2010 / Published online: 8 December 2010
© Springer Science+Business Media, LLC 2010

ABSTRACT

Purpose To investigate the possibility of using localized nucleic drug delivery methods for the treatment of osteolysis-related bone disease.

Methods A bio-degradable cationic hydrogel composed of gelatin and chitosan was used to deliver an antisense oligonucleotide (ASO) targeting murine TNF- α for the treatment of endotoxin-induced osteolysis.

Results ASO combined with this hydrogel was released when it was digested by adhering cells. The released ASO was efficiently delivered into contacted cells and tissues *in vitro* and *in vivo*. When tested in animal models of endotoxin-induced bone resorption, ASO delivered by such means effectively suppressed the expression of TNF- α and subsequently the osteoclastogenesis *in vivo*. Osteolysis in the endotoxin-induced bone resorption animal models was blocked by the treatment.

Conclusion This is a successful attempt to apply localized gene delivery method to treat inflammatory diseases *in vivo*.

KEY WORDS antisense · localized gene delivery · osteolysis · TNF- α

INTRODUCTION

The basic premise of somatic gene therapy is that nucleic drug can be used to alter *in vivo* expression of the targeted genes (1,2). Controlled efficient delivery technology for nucleic acid drug has implications in fields of basic research and clinical medicine (3,4). However, satisfactory delivery system that can be used for *in vivo* nucleic drug delivery is quite rare. As a potential candidate for the next generation of medication, nucleic drug needs the promotion from pharmaceutical research aimed at the *in vivo* delivery technology with high efficiency.

Nanoparticle-based delivery systems encountered great obstacles when used *in vivo* because of poor targeting effects (5–7). Attempts using ligand modification to improve the targeting delivery ability of nanoparticles only achieved some uncertain results in most cases (8,9). The plausible theory of ligand/receptor-directed delivery proved its validity when tested *in vitro*. However, when injected into the body, ligand-modified nanoparticles cannot really escape from the infiltration system of the body and reach the right tissue and cell (10). On the contrary, complex modification increased the instability of the delivery systems, especially in physiological conditions. Additionally, the technological complexity in manufacture and subsequent high cost make it impossible to apply most of the technologies in industry (11).

Localized delivery systems for nucleic acid drug offer alternative strategies that exhibit much superiority over nanoparticles when used *in vivo* (12). The controlled delivery of from biodegradable materials maintains an elevated concentration of nucleic acid within the cellular microenvironment by supplying nucleic acid to balance the loss by degradation (13). The continued presence of the nucleic acid during cell division seems to facilitate entry into the

L. Dong · Z. Huang · X. Cai · J. Xiang · Y.-A. Zhu · J. Chen · J. Zhang
State Key Laboratory of Pharmaceutical Biotechnology
School of Life Sciences
Nanjing University
Nanjing 210093, China

J. Zhang (✉)
Jiangsu Provincial Diabetes Center, Nanjing University
Nanjing 210093, China
e-mail: jfzhang@nju.edu.cn

R. Wang
Department of Orthopaedics, Jinling Hospital, School of Medicine
Nanjing University
Nanjing 210093, China

cells and nucleus (14). When used *in vivo*, localized delivery systems could stably maintain a high concentration of nucleic acid at the sites where the systems were implanted and achieve effective transfections to the contacted tissues (15). Although these kinds of *in situ* delivery methods cannot be widely used for *in vivo* applications of nucleic drugs because of the limitation of their request of implantation, the effectiveness and stability offers them the potential to be introduced clinically for some special applications such as drug-eluting stent and cartilage gene-activated regenerative materials (16–18).

In the present study, a biodegradable cationic hydrogel composed of gelatin and chitosan was used to deliver an antisense oligonucleotide targeting murine TNF- α for the treatment of endotoxin-induced osteolysis. Our previous study demonstrated that silencing TNF- α by antisense nucleotide effectively alleviated osteolysis induced by particle wear from Co-Cr-Mo alloy (19). Because aseptic loosening is a local chronic inflammation, a localized controlled release system was designed and developed in order to enhance the ASO's efficacy and prolong its effect.

MATERIALS AND METHODS

Materials

Chitosan (MW 350KDa, >90% deacetylated), gelatin B powder (from bovine skin) and Lipopolysaccharide (LPS, *Escherichia coli* 0127:B8) were purchased from Sigma-Aldrich Co. (St. Louis, MO, USA). *N*-(3-dimethylaminopropyl)-*N*-ethyl -carbodiimide (EDC), *N*-hydroxysuccinimide (NHS) and 2-morpholinoethane sulfonic (MES) were purchased from Amersco Company (USA). Transfection reagent Lipofectamine 2000™ was purchased from Invitrogen. The TNF- α ELISA kit was purchased from eBioscience Co. (San Diego, CA, USA). All other reagents were of analytical grade and were used as received.

The phosphorothioate-modified ASO used in this study, ISIS-25302, was synthesized by TAKARA (Dalian, China). For cell treatment, the ASO was sterilized by filtration through 0.22 μ m filter and stored at -70°C prior to use. The sequence of ISIS-25302 is 5'-AACCCATCGGCTGG CACCAC-3'. It was designed to target the primary RNA transcript of TNF- α and was found to strongly inhibit the TNF- α production (20).

Cells and Animals

RAW 264.7 cells were cultured in Dulbecco's Modified Eagle Medium (DMEM medium containing 10% heat-inactivated fetal bovine serum, and maintained in humidified 5% CO₂ incubator at 37°C before use).

Female SD rats and C57/BL6 mice were purchased from the Experimental Animal Centre of Nanjing Medical University (Nanjing, China) and maintained under barrier conditions and were pathogen-free as assessed by regular microbiologic screening.

Preparation of Gelatin-Chitosan-ASO (GCA) Systems

Gelatin B and chitosan (weight ratio of 1:1) were dissolved in 1% acetic acid to a final concentration of 10 mg/ml. The required volume of this solution was heated to dry in a dish to form a film with a thickness of 0.2 mm. After that, this dish was filled with 5 M NaOH to neutralize the acetic acid remnant and strengthen the film. The NaOH was washed away in flowing water. The film is a hydrogel which could swell in water and be stripped from the dish. Then, the swelling hydrogel was dehydrated and kept in 90% ethanol, which also helped to sterilize the film.

To load ASO and obtain the GCA, the dehydrated hydrogel film was swelling in ASO solution which was sterile-filtered through a 0.22 μ m filter. The loaded amount of ASO could be calculated from the weight difference between the dehydrated hydrogel and the swelling hydrogel according to the concentration of ASO solution. Change the concentration of ASO solution can change the drug loading rate of the hydrogel.

Cell Culturing and Transfections

RAW 264.7 cells were seeded in a six-well plate covered with GCA films at an initial density of 5×10^5 cells per well in 2 ml DMEM. The cell was removed from the GCA films by trypsin digestion, washed in PBS three times and quantified for its ASO content. As a control, transfection with Lipofectamine 2000 using the same amount of ASO as in GCA was performed in accordance with the manufacturer's instructions. Naked ASO and ASO/chitosan complex were also use as controls in the experiment.

Scanning Electron Microscopy

For scanning electron microscopy (SEM) analysis, samples cultured with cells were fixed in a glutaraldehyde solution in PBS (2% *w/v*, 4°C) for at least 24 h. Thereafter, samples were dehydrated in a graded series of ethanol and air-dried. Samples without cells were used directly. After sputter-coating with gold/palladium (10 nm), the samples were examined using an S-3400 N SEM (Hitachi, Japan).

DNA Release

An appropriate amount of ASO was loaded onto each piece of film in a six-well plate, and, with or without

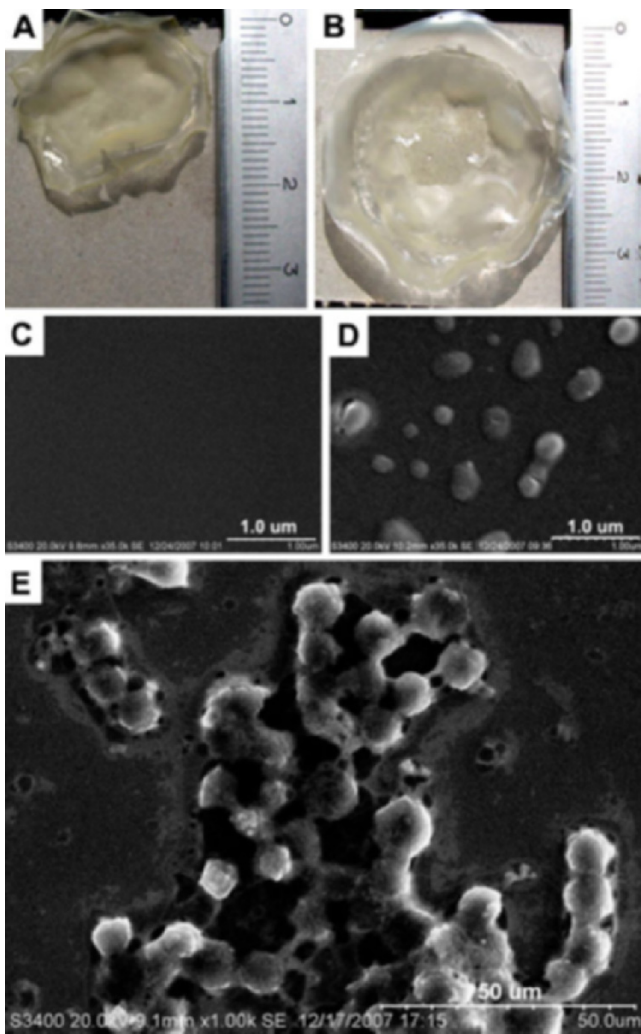


Fig. 1 Morphological studies of the GCA system. **A** dehydrated GCA; **B** swelling GCA; **C** SEM photograph of gelatin-chitosan hydrogel without ASO; **D** SEM photograph of GCA; **E** SEM photograph of GCA digested by cultured cells.

cultured cells, the film was incubated with 2 ml complete DMEM. At various time points, 1 ml supernatant was collected, and the volume was supplemented by fresh medium. The amount of ASO in supernatant was quantified.

Quantification of ASO in Cells and in Supernatant

The ASO was extracted from transfected cells and supernatant collected at different time points. Then, the extracted ASO was separated by electrophoresis in 20% polyacrylamide denaturing gel containing 7 M urea. The separated ASO in gel was transferred to Hybond nylon membrane (Amersham Pharmacia Biotech) and then cross-linked by UV irradiation. The membrane was prehybridized in tube for 2 h at 40°C in prehybridization buffer and

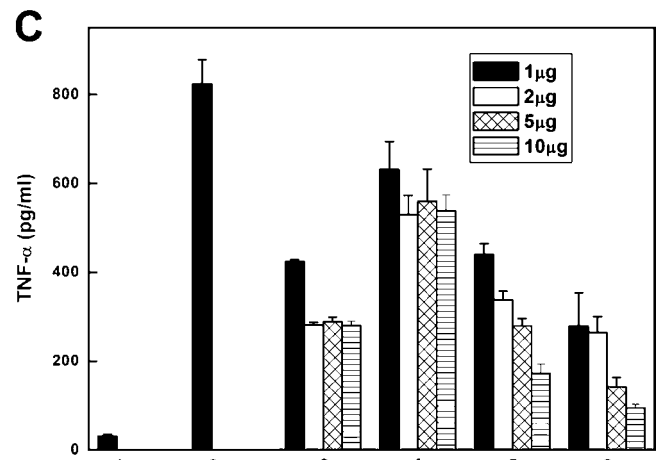
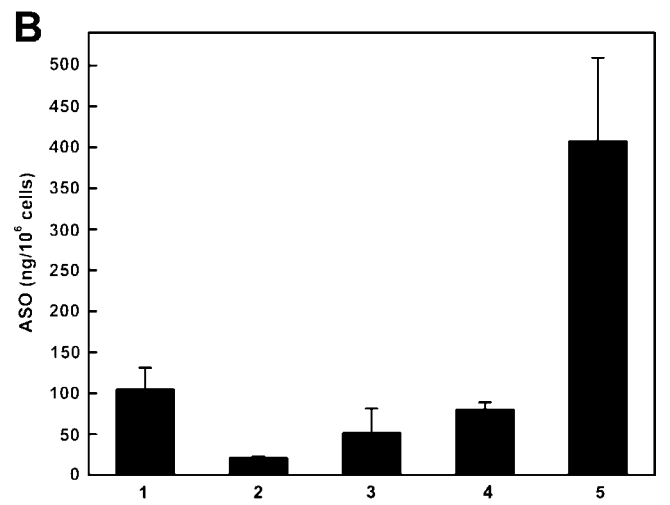
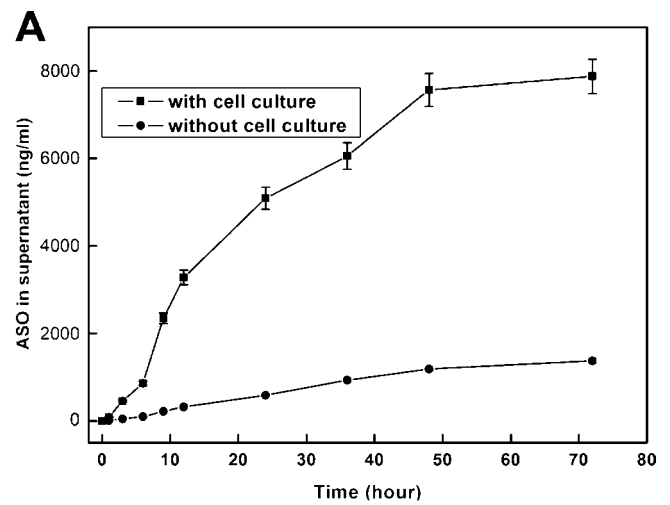


Fig. 2 ASO release, the transfection efficiency and the effect of the transfected ASO. **A** ASO release in cell culture or without cell culture; **B** ASO transfected into raw 264.7 cells by (1) lipofactamin 2000, (2) Naked ASO, (3) gelatin, (4) chitosan and (5) GCA system; **C** the suppression on the expression of TNF-α by ASO. (1) controlled cell culture supernate; (2) cell culture stimulated with LPS and without ASO treatment; (3) cell culture stimulated with LPS and the ASO was delivered by lipofectamine 2000; (4) cell culture stimulated with LPS and treated by naked ASO; (5) cell culture stimulated with LPS and treated by chitosan-delivered ASO; (6) cell culture stimulated with LPS and treated by GCA system.

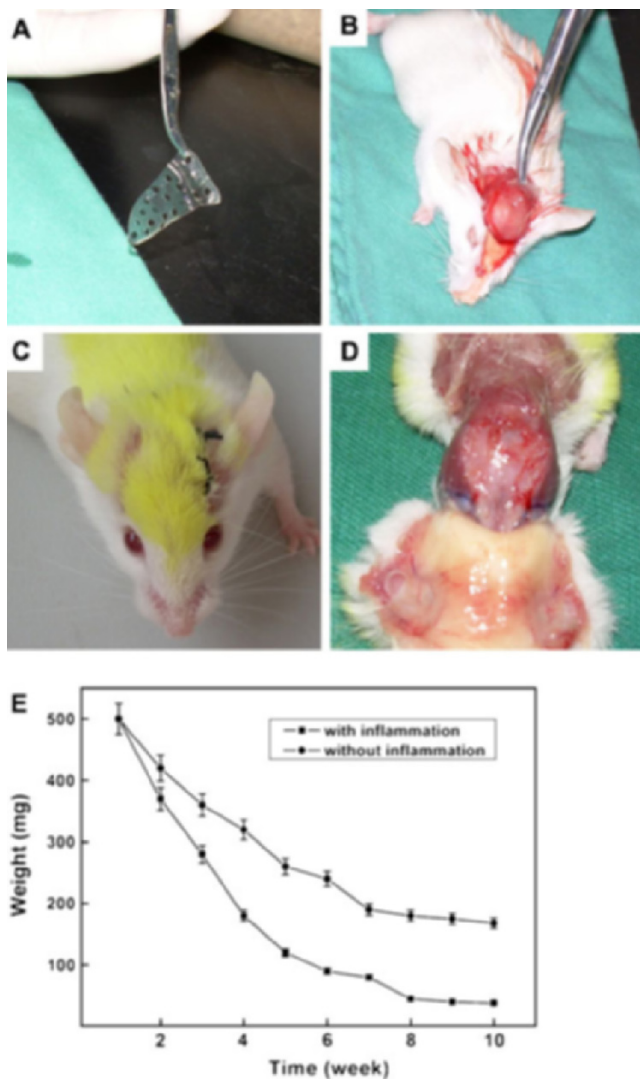


Fig. 3 The *in vivo* experimental process. **A** cribriform GCA hydrogel film; **B** place the GCA film onto the calvarium of the animal; **C** the skin was sewed up after operation; **D** GCA hydrogel was digested and absorbed 2 months after implantation; **E** the digestion rate of GCA hydrogel *in vivo* under normal conditions and inflammatory conditions.

hybridized for 4 h at 40°C in fresh hybridization buffer containing ^{32}P -labeled sense oligonucleotides. Following hybridization, the membrane was sequentially washed in $5\times$ standard saline citrate (SSC) buffer and $5\times$ SSC/0.05% SDS buffer for 20 min at 40°C, respectively. The membrane was exposed to phosphor screen overnight at room temperature. The autoradiograms were scanned, and the densities associated with bands were compared using the Packard Cyclone Storage Phosphor System (Packard Instrument Company, Inc., USA). In each hybridization another membrane containing a different amount of the standard ASO was also included. The amount of the unknown was extrapolated from the standard curve (21).

TNF- α Expression Assay

TNF- α expression was analyzed by ELISA assay. The cells after transfection were stimulated by LPS (500 ng/ml, 4 h). The culture supernatants were collected at the end of the stimulation of LPS and were examined by ELISA kit according to the manufacturer's instructions. Samples were run in triplicate and were diluted appropriately to make sure that TNF- α values were within the range of the standard curve.

Endotoxin-Induced Bone Resorption Mouse Model (EIBR)

Endotoxin-induced bone resorption mouse model was performed according to an established method (22,23). Seven-to-eight-week-old mice were administered a local calvarial injection of lipopolysaccharide (LPS) at 25 mg/kg ($n=10$). GCA systems were implanted on the calvaria by operation. The GCA systems loaded with a controlling mismatched ASO were used as the control. LPS was given to the animals every week. After 4 weeks, osteoclast numbers per square millimetre of trabecular bone surface and the bone resorptions were measured (24). To evaluate the *in vivo* transfection effect of GCA, a rhodamine-labeled ASO was loaded in GCA. The periosteum of calvaria separated from the animals implanted with GCA loaded with rhodamine-labeled ASO was frozen and sectioned to examine the transfected ASO.

Statistical Analysis

Data are expressed as means \pm SD. Statistical significance was determined by one-way analysis of variance (ANOVA) with multiple comparison of Tukey, where $p < 0.05$ was considered statistically significant.

RESULTS

Morphological Studies

The gelatin/chitosan hydrogel films prepared by using our protocol have a relatively strong mechanical strength, which made the hydrogel easily shaped to facilitate the *in vitro* and *in vivo* application. The hydrogel could swell in water and become about six times as large as its volume (Fig. 1A and B). When loaded with ASO, a lot of particle-like structures could be found in the surface of the film by using SEM observation, while non-loading film did not show such morphology (Fig. 1C and D). The gelatin/chitosan hydrogel could support the attachment and growth of the cell. More importantly, the hydrogel could be effectively eroded by the growing cells, which may be due to the digestion of enzymes in extracellular matrix (ECM) (Fig. 1E).

ASO Release, Transfection Efficiency, and Effect of Transfected ASO

GCA hydrogel could slowly release ASO into the cell medium. About 5% of the total ASO (20 μg) contained in the GCA was released into the medium in 72 h. Raw 264.7 cells seeded on the hydrogel notably exceeded the release rate of ASO. About 40% of the total ASO was released into the medium in 72 h.

The ASO transfection effect was examined on a GCA hydrogel containing 5 μg ASO. The same amount of ASO transfected by lipofectamine 2000, chitosan or just naked ASO was tested simultaneously as the controls. The result was shown in Fig. 2B. GCA delivered ASO into the cells with much higher efficiency than lipofectamine 2000 and chitosan after 48 h.

We transfected RAW cells with different amounts of ASO and stimulated the cells with LPS by the same concentration and time 24 h after transfection. After LPS stimulation, non-transfected cells produced more than 20-fold increased amount of TNF- α (824 pg/ml) compared to the control (32 pg/ml). Naked ASO had some effect of inhibition (30–40%), but increased amount of ASO could not improve the silencing ability. Lipofectamine 2000 could silence the expression of TNF- α by half when 1 μg ASO was used. The rate of inhibition rose to about 60% as ASO was added up to 2 μg . After that, it remained invariant despite the increment of ASO. In contrast to Lipofectamine2000, chitosan/ASO presented different characteristics. At lower concentration of ASO, consistent effect was obtained as that of Lipofectamine2000, but when ASO was increased, the rate of inhibition went up together and

exceeded that of Lipofectamine2000 at the highest amount of ASO. In the group of GCA, 10 μg of ASO had almost thoroughly inhibited the expression of TNF- α , and the amount of TNF- α was almost equal to blank control which had no LPS stimulation.

GCA Suppressed the Osteoclastogenesis and Bone Resorption in EIBR Animal Model

The *in vivo* experimental process is shown in Fig. 3A–D. Small holes were made in the GCA films used in the animal experiments to facilitate the healing of the opening skin over the skull (Fig. 3A). The GCA film was placed over the calvarium, and the skin was sewn up (Fig. 3B and C). A 500-mg GCA film can be digested and absorbed within 10 weeks. No obvious inflammatory symptoms were observed in the calvarial tissues (Fig. 3D). The digestion rate was measured and calculated in Fig. 3E. When the animal was under a controlled inflammatory condition stimulated by injected LPS, the GCA film was absorbed more quickly and thoroughly.

ASO delivered by GCA system more efficiently entered the contacted tissue compared to the naked ASO (Fig. 4A–C) 72 h after it was implanted. Because of the LPS stimulation, the expression of several important cytokines including TNF- α was up-regulated in EIBR animal. Anti-TNF- α ASO delivered by GCA systems effectively suppressed the expression of TNF- α , M-CSF and RANKL. Naked ASO has little suppression effects.

M-CSF and RANKL are key factors in osteoclastogenesis. Enhanced concentration of these two cytokines

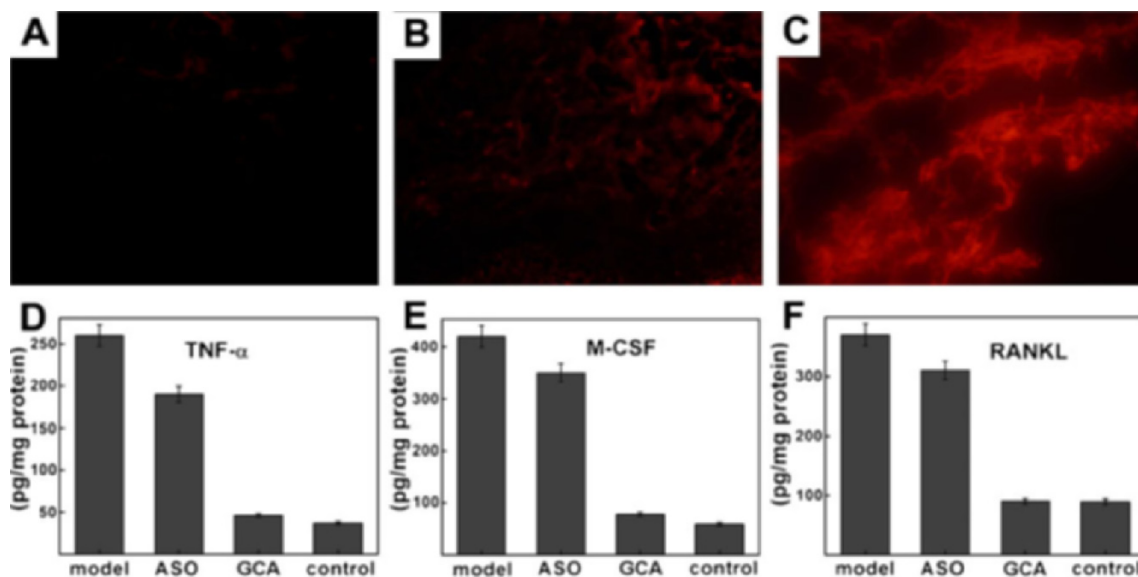


Fig. 4 *In vivo* transfection effect of GCA system and its suppression on inflammatory cytokines. **A** frozen section of controlled periosteum tissue; **B** frozen section of periosteum tissue separated from animal injected with naked rhodamine-labeled ASO; **C** frozen section of periosteum tissue separated from animal implanted with GCA containing rhodamine-labeled ASO; **D** TNF- α concentrations in the periosteum tissues of animals with different treatment; **E** M-CSF concentrations; **F** RANKL concentrations. All samples were harvested 4 weeks after GCA or naked ASO was given to the animal. $P < 0.001$.

resulted in the increased osteoclastogenesis level (Fig. 5A). Increased osteoclasts resorbed some bone tissue in the calvaria to form osteolysis lacunas which can be stained by toluidine blue (Fig. 5E). ASO delivered by GCA systems can notably decrease the osteoclastogenesis level (Fig. 5B) and subsequently the osteolysis degree (Fig. 5G). As the control, naked ASO has little influence on the EIBR animal model (Fig. 5I and J). All the data was obtained eight weeks after the GCAs were implanted in to the animals.

DISCUSSIONS

TNF- α is a key element in osteoclastogenesis processes occurring in arthritis and other inflammatory bone diseases, such as aseptic loosening (25,26). In our previous studies, anti-TNF- α ASO was used to inhibit the metal particle-induced osteolysis, which is an animal model of aseptic

loosening (19). In that study, naked ASO was directly injected into the inflammation sites in the calvaria. This is also a kind of localized delivery of ASO because the structure of the skin and skull to form a relatively enclosed space limited the diffusion of the drug and maintained a relatively high concentration in the infected sites, which supplied a good transfection efficiency *in vivo*. Within two weeks, injected ASO exhibited effective inhibition both in osteoclastogenesis and bone resorption.

In most cases, osteoclastogenesis-related bone resorption occurs in chronic diseases such as rheumatoid arthritis, osteoarthritis, osteoporosis and aseptic loosening (27–30). This requires the drugs to have long-term efficacy. To achieve such a prolonged acting-time of the ASO, a controlled release system, GCA was developed. The GCA system must have the ability to combine and control the release the ASO as well as guarantee the transfection efficiency. Another important property of the system is it

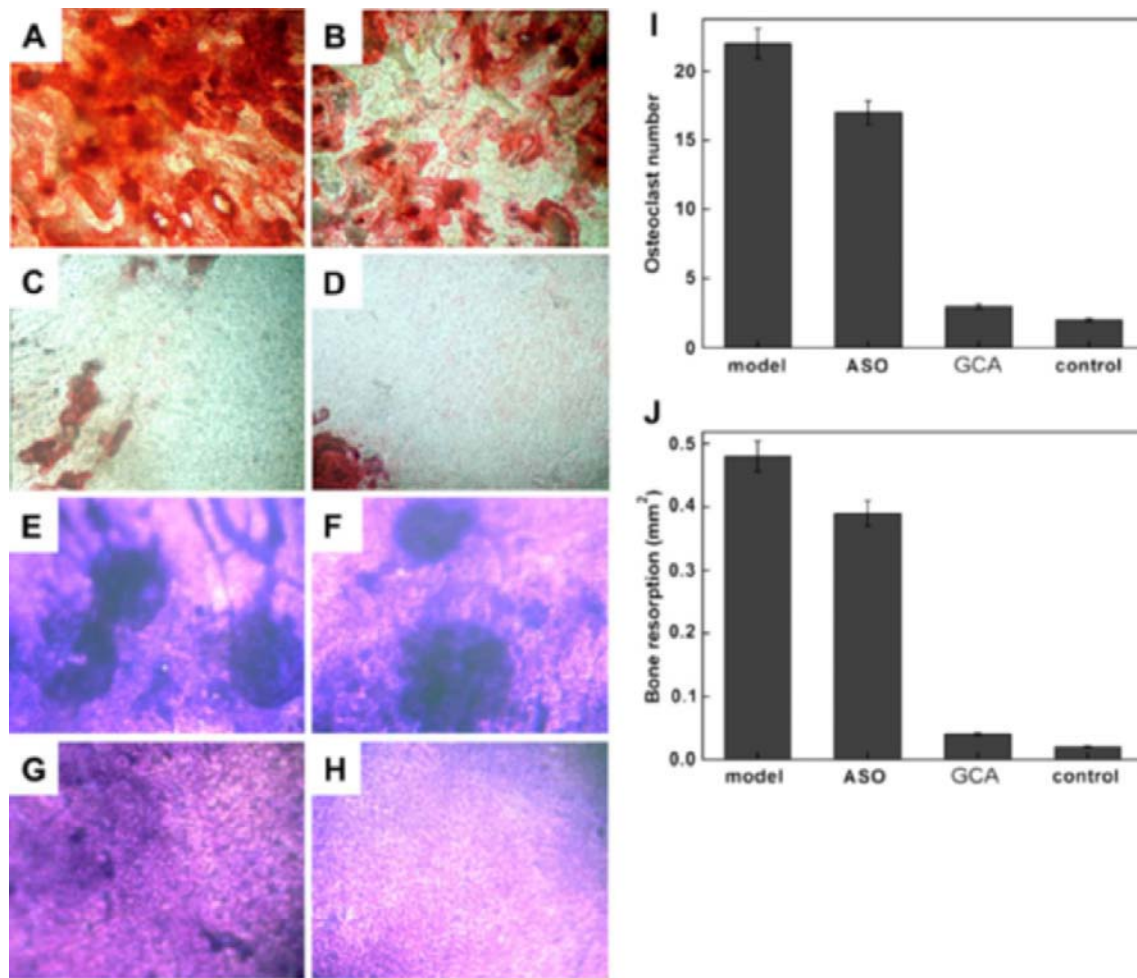


Fig. 5 Effects of GCA on the osteoclastogenesis and osteolysis of EIBR animal models. **A** osteoclasts on the calvarium of EIBR mouse; **B** osteoclasts on the calvarium of EIBR mouse treated with naked ASO; **C** treated with GCA; **D** healthy animal control; toluidine blue stained bone resorption lacuna of **E** EIBR animal model; **F** EIBR animal treated with naked ASO; **G** EIBR animal treated with GCA; **H** healthy animal; **I** osteoclast number count; **J** calculation of bone resorption lacuna. All samples were harvested 8 weeks after GCA was given to the animals. $P < 0.001$.

should have good biocompatibility to facilitate its application *in vivo*. The components of the system, chitosan and gelatin, gave the system biodegradability, low toxicity and low immunogenicity. In our experiment, the preparation of this delivery system did not include any chemical modification processes or introduce any other reagents to this system to change its toxicity. Additionally, no parent toxicity was observed in the cellular experiments and animal tests performed in our present study. As a cationic polysaccharide, chitosan offered the system the ability to combine negative-charged ASO. Gelatin was easier to digest *in vivo* than chitosan. The GCA film was broken down with the digestion of the gelatin components in GCA. In the meantime, chitosan/ASO complex was released and taken by the closely contacting tissue and cells. This is a typical localized gene delivery method, which satisfied *in vivo* transfection efficiency in this study.

The application of localized gene delivery *in vivo* is very limited. The main reason is that this kind of gene delivery method needs an artificial surface to control release of nucleotides and to contact with targeted cells and tissues. This kind of surface is easy to obtain in cellular experiments *in vitro* but is difficult to use *in vivo*. The solid holder of nucleotide needs to be implanted into the body by surgical operation. Moreover, there are very limited kinds of pathological structures that are suitable to treat with a gene-releasing implant. Additionally, the key property of localized gene delivery method is the requirement of full contact between targeted cells and the gene-bearing surface. This is difficult *in vivo* when an organ or piece of tissue needs to be transfected because the implant number is limited and it can only contact very few cells in such conditions. Gene-driving cartilage regenerative scaffold and nucleotide drug-eluting stent are some of the successful applications of the localized gene delivery method *in vivo*. To achieve wider application of such method, the gene-bearing implant must be modified in two aspects: easy to use and have some dispersity to facilitate it to contact enough cells *in vivo*. Though in the present study, we still used a solid implant to contact the pathologic tissue and to control the release of the nucleotide, the hydrogel nature of the implant has the potential to be transformed into an injectable material with high dispersity such as injectable hydrogel or microspheres. In our other study, a kind of injectable cationic hydrogel was developed and used to treat rheumatoid arthritis by delivery of ASO to the immune cells (31).

In conclusion, the present study attempted to apply the localized gene delivery method to treat diseases *in vivo*. This strategy exhibited satisfactory therapeutic effect by using antisense nucleotide. Its hydrogel nature makes it have the potential to be transformed into preparations which are injectable and have enough dispersity to be used widely in other diseases.

REFERENCES

1. Verma IM, Weitzman MD. Gene therapy: twenty-first century medicine. *Annu Rev Biochem.* 2005;74:711–38.
2. Mulligan RC. The basic science of gene therapy. *Science.* 1993;260:926–32.
3. Shoji Y, Nakashima H. Current status of delivery systems to improve target efficacy of oligonucleotides. *Curr Pharm Des.* 2004;10:785–96.
4. Weyermann J, Lochmann D, Zimmer A. Comparison of antisense oligonucleotide drug delivery systems. *J Control Release.* 2004;100:411–23.
5. Mok H, Park TG. Functional polymers for targeted delivery of nucleic acid drugs. *Macromol Biosci.* 2009;9:731–43.
6. Mahato RI, Takakura Y, Hashida M. Development of targeted delivery systems for nucleic acid drugs. *J Drug Target.* 1997;4:337–57.
7. Ye X, Yang D. Recent advances in biological strategies for targeted drug delivery. *Cardiovasc Hematol Disord Drug Targets.* 2009;9:206–21.
8. Hughes JA, Rao GA. Targeted polymers for gene delivery. *Expert Opin Drug Deliv.* 2005;2:145–57.
9. Gary DJ, Puri N, Won YY. Polymer-based siRNA delivery: perspectives on the fundamental and phenomenological distinctions from polymer-based DNA delivery. *J Control Release.* 2007;121:64–73.
10. Petros RA, DeSimone JM. Strategies in the design of nanoparticles for therapeutic applications. *Nat Rev Drug Discov.* 2010;9:615–27.
11. Oupicky D, Konak C, Ulbrich K, Wolfert MA, Seymour LW. DNA delivery systems based on complexes of DNA with synthetic polycations and their copolymers. *J Control Release.* 2000;65:149–71.
12. Pannier AK, Shea LD. Controlled release systems for DNA delivery. *Mol Ther.* 2004;10:19–26.
13. Park TG, Jeong JH, Kim SW. Current status of polymeric gene delivery systems. *Adv Drug Deliv Rev.* 2006;58:467–86.
14. Tseng WC, Haselton FR, Giorgio TD. Mitosis enhances transgene expression of plasmid delivered by cationic liposomes. *Biochim Biophys Acta.* 1999;1445:53–64.
15. Ochiya T, Takahama Y, Nagahara S, Sumita Y, Hisada A, Itoh H, *et al.* New delivery system for plasmid DNA *in vivo* using atelocollagen as a carrier material: the Minipellet. *Nat Med.* 1999;5:707–10.
16. Wessely R. New drug-eluting stent concepts. *Nat Rev Cardiol.* 2010;7:194–203.
17. Guo T, Zhao J, Chang J, Ding Z, Hong H, Chen J, *et al.* Porous chitosan-gelatin scaffold containing plasmid DNA encoding transforming growth factor-beta1 for chondrocytes proliferation. *Biomaterials.* 2006;27:1095–103.
18. Diao H, Wang J, Shen C, Xia S, Guo T, Dong L, *et al.* Improved cartilage regeneration utilizing mesenchymal stem cells in TGF-beta1 gene-activated scaffolds. *Tissue Eng A.* 2009;15:2687–98.
19. Dong L, Wang R, Zhu YA, Wang C, Diao H, Zhang C, *et al.* Antisense oligonucleotide targeting TNF-alpha can suppress Co-Cr-Mo particle-induced osteolysis. *J Orthop Res.* 2008;26:1114–20.
20. Myers KJ, Murthy S, Flanigan A, Witchell DR, Butler M, Murray S, *et al.* Antisense oligonucleotide blockade of tumor necrosis factor-alpha in two murine models of colitis. *J Pharmacol Exp Ther.* 2003;304:411–24.
21. Dong L, Gao S, Diao H, Chen J, Zhang J. Galactosylated low molecular weight chitosan as a carrier delivering oligonucleotides to Kupffer cells instead of hepatocytes *in vivo*. *J Biomed Mater Res A.* 2008;84:777–84.

22. Ukai T, Hara Y, Kato I. Effects of T cell adoptive transfer into nude mice on alveolar bone resorption induced by endotoxin. *J Periodontol Res.* 1996;31:414–22.
23. Sakuma Y, Tanaka K, Suda M, Komatsu Y, Yasoda A, Miura M, et al. Impaired bone resorption by lipopolysaccharide *in vivo* in mice deficient in the prostaglandin E receptor EP4 subtype. *Infect Immun.* 2000;68:6819–25.
24. Dong L, Xia S, Gao F, Zhang D, Chen J, Zhang J. 3, 3'-Diindolylmethane attenuates experimental arthritis and osteoclastogenesis. *Biochem Pharmacol.* 2010;79:715–21.
25. Ritchlin CT, Haas-Smith SA, Li P, Hicks DG, Schwarz EM. Mechanisms of TNF-alpha- and RANKL-mediated osteoclastogenesis and bone resorption in psoriatic arthritis. *J Clin Invest.* 2003;111:821–31.
26. Schwarz EM, Looney RJ, O'Keefe RJ. Anti-TNF-alpha therapy as a clinical intervention for periprosthetic osteolysis. *Arthritis Res.* 2000;2:165–8.
27. Ochi S, Shinohara M, Sato K, Gober HJ, Koga T, Kodama T, et al. Pathological role of osteoclast costimulation in arthritis-induced bone loss. *Proc Natl Acad Sci USA.* 2007;104:11394–9.
28. Shibakawa A, Yudoh K, Masuko-Hongo K, Kato T, Nishioka K, Nakamura H. The role of subchondral bone resorption pits in osteoarthritis: MMP production by cells derived from bone marrow. *Osteoarthritis Cartilage.* 2005;13:679–87.
29. Lazner F, Gowen M, Pavasovic D, Kola I. Osteopetrosis and osteoporosis: two sides of the same coin. *Hum Mol Genet.* 1999;8:1839–46.
30. Greenfield EM, Bi Y, Ragab AA, Goldberg VM, Van De Motter RR. The role of osteoclast differentiation in aseptic loosening. *J Orthop Res.* 2002;20:1–8.
31. Dong L, Xia S, Chen H, Chen J, Zhang J. Spleen-specific suppression of TNF-alpha by cationic hydrogel-delivered anti-sense nucleotides for the prevention of arthritis in animal models. *Biomaterials.* 2009;30:4416–26.